Proceedings World Geothermal Congress 2015
Melbourne, Australia, 19-25 April 2015

Mapping of Hydraulic Fractures Using Tiltmeter Data for Design of EGS Stimulation

Pandurangan, V., Chen, Z. R., Jeffrey, R.G

CSIRO Earth Science and Resource Engineering, Melbourne, Victoria, Australia
Venkataraman.pandurangan@csiro.au

Keywords: Asymmetric fractures, tiltmeter, displacement discontinuity, Extended Kalman filter

ABSTRACT

Tiltmeters are widely used in the monitoring of hydraulic fractures, a procedure wherein reservoir rock formations are fractured by the injection of pressurized fluid to enhance well productivity. Tiltmeters measure the fracture induced deformations which can then be inverted to obtain useful fracture parameters. Hydraulic fracturing is now being proposed for stimulation of enhanced geothermal systems in low permeability rock for increased energy extraction. Small scale field sites are proposed as a method to obtain data on the effect of placing multiple hydraulic fractures in an injection well and connecting them to a production well. Fracture growth parameters obtained from tiltmeter mappings at such experiment sites can be used to study the effectiveness of such stimulations. In this work, we propose an approach for the inversion of tilt data using the displacement discontinuity method and the extended Kalman filter. The salient feature of the proposed method is its ability to predict fracture asymmetry with respect to the injection borehole, which is important to know to determine if each stimulation in an array has progressed as expected. This approach uses a forward model based on the analytical solution for computing the displacements and tilts due to a point source displacement discontinuity in an elastic half-space which was developed by Okada (Okada, 1992). The displacement and tilts for any given fracture geometry are then obtained by numerical integration of this solution, by considering multiple point sources to be located at the quadrature points. The proposed method is validated using synthetic data sets generated from polygon and elliptical shaped fracture geometries. Finally, real data obtained from a field site (but not a geothermal site) has also been analyzed. Preliminary results show that the procedure is able to satisfactorily predict fracture geometrical parameters when the fracture is relatively close to the tiltmeter.

1. INTRODUCTION

In geothermal reservoirs optimal heat extraction is important for the energy extraction to be economical. For this to happen, the reservoir must have sufficiently high permeability to ensure large enough fluid circulation rates to promote convective heat transfer between the hot rock and the injected fluid at a rate that is economic. However, in many geothermal fields the rock mass has high temperature but very low permeability that is insufficient to maintain enough fluid circulation for useful energy extraction. Enhanced geothermal systems (EGS), addresses this issue by artificially increasing the permeability of the rock mass through external stimulation. The stimulation helps to increase the permeability and creates additional pathways for the fluid to flow, resulting in improved heat exchange and higher productivity (Tester et al., 2006). Commonly used stimulation methods include, hydraulic fracturing in which a high pressure fracturing fluid with or without proppants is injected into the rock formation to create fractures (Economides and Nolte, 2000), hydro-shearing wherein a lower pressure fluid is used to promote shear-induced dilation in the naturally fractured rocks (Riahi and Damjanac, 2013), or chemical stimulation that uses acids or solvents to treat the regions close to the well bore or to remove material deposits in the existing fractures (Portier et al., 2009). In all these methods, the end objective is to ensure that fracture conductivity is created and maintained to ensure enough fluid circulation can be achieved for effective heat extraction.

The hydraulic fracturing technique has been used in oil and gas well stimulation since the late 1940s and recently has also been used as a preconditioning method to promote earlier and more continuous caving in underground coal and metal mines (Jeffrey et al., 2013). Micro seismic event location and tilt measurements are commonly used to monitor the growth of hydraulic fractures to ensure the effectiveness of the fracturing treatment and avoid fracture growth into environmentally sensitive regions. Tiltmeters are instruments with sensors that are sensitive to small changes in inclination along two orthogonal directions. They can therefore be used to measure the deformation at the surface (surface tiltmeter technique) or in the interior (downhole tiltmeter technique) of the earth due to the propagation of hydraulic fractures. This information is used to obtain fracture parameters such as dip, strike and volume, and occasionally the fracture geometry by inverse mapping. To carry out inverse mapping a forward model capable of predicting the displacement and tilts caused by a fracture is required. Forward models based on the distributed displacement discontinuity (DD) technique have been successfully used for tiltmeter mapping of hydraulic fractures (Lecampion and Gunning, 2007). However, many of the forward models based on the DD technique approximate the propagating fracture by simple geometric shapes such as a rectangle or a square and therefore can provide only limited geometric information about the fracture upon inversion. Another problem encountered in hydraulic fracturing is the possibility of the fractures developing asymmetrically with respect to the wellbore. Asymmetrically developed fracture growth has been shown to significantly affect production rates and fracture conductivity or how fast the fluid mixed with proppant flows through the fracture. In a worst case it may make the fracturing treatment ineffective and not have any effect on improving productivity (Bennett et al., 1983). Asymmetric fracture development also influences the design of optimal well patterns during recovery operations (Rodriguez et al., 1992), and further if the asymmetry occurs during pumping it can result in a screen out where the injection pressure exceeds safe operating pressures (Jeffrey, 1996). Accounting for asymmetry is important in assessing the effectiveness of hydraulic fracture stimulation when used in applications such as the preconditioning of rock mass. In the case of multiple hydraulic fractures, asymmetric growth of one fracture can affect the stress field around it and can thereby influence the growth of the next fracture as well (Jeffrey et al., 2013; Kear et al., 2013).

When using symmetric DD models, an additional parameter known as the center offset is used to quantify the movement of fracture center as asymmetry develops. The center offset is not known a priori and has to be estimated by inversion and any error in

estimating the offset can have an impact on the accuracy of the predicted fracture dip and dip orientation (Jeffrey et al., 2013). To address this issue, we propose a forward model that considers asymmetric crack growth with respect to the injection point. The fracture center offset need not be estimated in this case. The forward model also provides a numerical solution for general polygonal shaped fracture geometry, as an approximation for a real fracture that grows with a non-circular shape. Hence, the inversion can provide more realistic information on the geometry of the developing fracture. The other improvement proposed in the present method is the use of a modified extended Kalman filter for the inverse mapping. In inverse mapping using a Bayesian approach (Lecampion and Gunning, 2007), the inversion of tiltmeter data is carried out discretely at every time step and does not consider the evolution of the fracture parameters with time or in other words the relationship between the fracture parameters between consecutive time steps. The extended Kalman filter allows the state of the system to be explicitly described using a set of linear or non-linear equations and information about fracture parameter evolution can be built into the system. Even when the precise model to describe the system dynamics is not available, the filter can still relate the fracture parameters at different time steps and therefore provide better estimates of the state vector. In a Bayesian sense this can be seen as additional prior information that can further help to constrain the solution space.

The remainder of the paper is organized as follows. Following this introduction, section 2 presents the theoretical background of the forward model and the modified extended Kalman filter used for the inverse mapping. In section 3, the results obtained by inverting synthetic and field data sets are presented, wherein the synthetic data sets are used for validating the model after which it is used to analyze data from an actual field experiment.

2. THE FORWARD MODEL AND INVERSION PROCEDURE

To analyze the tiltmeter data and obtain useful fracture parameters by inversion we need an appropriate forward mathematical model that can predict the displacement and tilt induced by a fracture, and an appropriate numerical scheme to carry out the inversion. In the current work the forward model is based on the displacement discontinuity method and the modified extended Kalman filter is used for inverting the data or in other words for finding a forward model that closely fits the data. In this section both the forward model and the modified extended Kalman filter are discussed in detail.

2.1 Displacement discontinuity method

The displacement discontinuity (DD) method is a boundary element method where, in the implementation used here, the fracture plane is discretized using constant displacement discontinuity elements of finite length. A displacement discontinuity can be visualized as a line crack in the x-y plane of the solid, whose opposite faces have been displaced from one another (Crouch and Starfield, 1983). The DD method is based on the concept of nuclei of strain that was initially proposed by Love (Love, 2013). It is based on the idea that the displacements and strains in an elastic, homogeneous and isotropic medium due to a displacement jump or discontinuity can be determined from the knowledge of fundamental solutions. The fundamental solutions are singular solutions to a point disturbance of any given orientation in an infinite or semi-infinite region. As the closed-form analytical solution for the displacements and strains due to a constant displacement discontinuity element in the x, y plane is known, the numerical solution for the displacement and strains due a given fracture geometry can be obtained by discretizing the fracture geometry into N constant displacement discontinuity elements and summing up the effects due to the individual elements using the principle of superposition. Although it is possible to model a fracture with a variable displacement jumps, assuming a constant value greatly simplifies the problem. An accurate solution then depends on using a fine enough discretization.

If we consider a planar fracture over the surface S, with a unit normal n and unit vector s along the fracture plane, and discretize it with constant DD elements, the displacements $\mathrm{u_i}$ at any point x in the medium, due to a DD singularity located at the point $\mathrm{x'}$, can be obtained using the principle of superposition as

$$\mathrm{u_i(x)} = \int_S \left\{\mathrm{U_{ijk}(x,x')n_i n_k D_n(x') + U_{ijk}(x,x')s_j n_k D_s(x')}\right\}\mathrm{ds} \quad (\mathrm{i,j,k} = 1,2,3) \tag{1}$$

where $\mathrm{U_{ijk}(x,x')}$ is the displacement tensor that represents the fundamental solution, $\mathrm{D_n} = \mathrm{D_{ij} n_i n_j}$ and $\mathrm{D_s} = \mathrm{D_{ij} s_i n_j}$ correspond to the normal and shear components of the displacement discontinuity respectively. The above integral is singular when $\mathrm{x} = \mathrm{x'}$ which is not an issue in tiltmeter mapping as the measurement points x are always located outside the fracture plane. The integral can be evaluated analytically or numerically depending on the problem complexity. The tilt components $\mathrm{w_1}$ and $\mathrm{w_2}$ at a given tiltmeter location is given by the curl of the displacement vector.

$$\mathrm{w_1} = \frac{\partial \mathrm{u_3}}{\partial \mathrm{x_1}} - \frac{\partial \mathrm{u_1}}{\partial \mathrm{x_3}}; \quad \mathrm{w_2} = \frac{\partial \mathrm{u_3}}{\partial \mathrm{x_2}} - \frac{\partial \mathrm{u_2}}{\partial \mathrm{x_3}} \tag{2}$$

A number of researchers have used the DD method to develop analytical expressions for the displacement, stresses and strains for radial, rectangular and penny shaped fractures (Converse and Comninou, 1975; Davis, 1983; Okada, 1985). The displacement discontinuity technique has mainly been used in constructing three-dimensional fracture models such as the solution for the displacement and tilt due to point displacements or rectangular fractures with a constant or variable opening in an elastic half-space or full space (Davis, 1983; Yang and Davis, 1986; Olson et al., 1997). However, these forward models use simple geometries such as a rectangle or square to represent the fracture geometry that may not accurately represent the actual fracture. As the DD singularity solution can be used to construct solution for any arbitrary shaped fracture geometry by using the principle of superposition, we propose a method for constructing the displacement and strain solution for a fracture with a general shape with more geometric features, which when used with an inversion procedure can provide a more realistic picture about the shape and size of the propagating fracture. As mentioned before, the model also considers the possibility of the fracture developing asymmetrically with respect to the borehole. Asymmetric fracture growth implies that the fracture grows predominantly along one direction with respect to the injection point. In this case, the forward model can use both symmetric and asymmetric shapes to approximate the fracture geometry. When the forward model uses a symmetric shape to represent the fracture geometry such as a rectangle, the asymmetry is accounted by a fracture center offset. As the current model considers the possibility of fractures propagating asymmetrically, a center offset is not required.

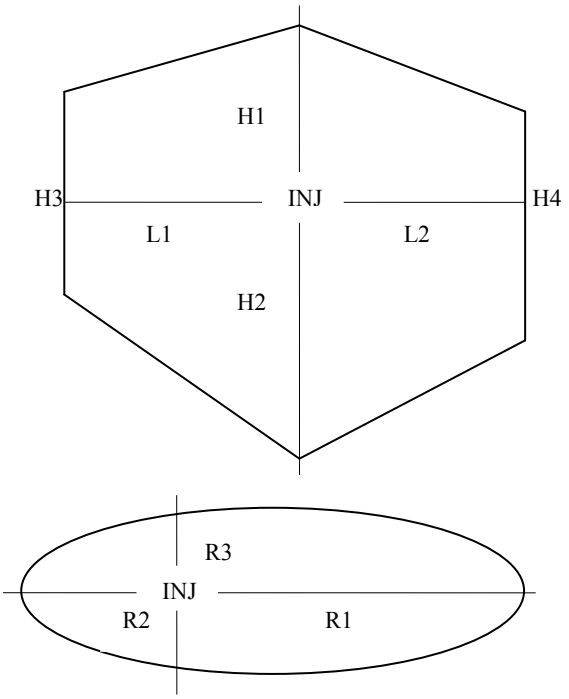

Figure 1 Geometric parameters of the polynomial and elliptical shaped DD model. (INJ refers to the injection point)

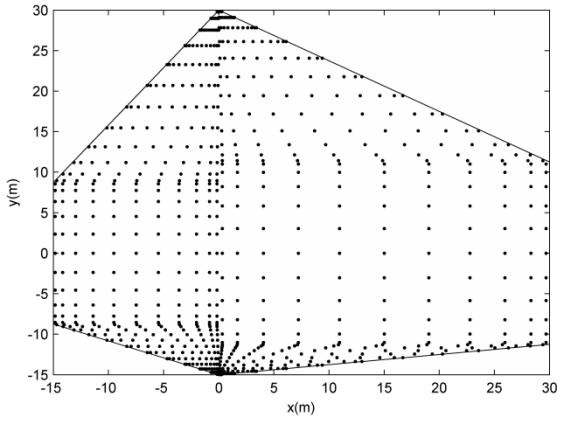

Figure 2 Distribution of quadrature points in the polygon Geometry.

In this work, the forward model is based on an elliptical and polynomial shaped displacement discontinuity in an elastic half space as shown in Figure 1. The fracture is allowed to propagate asymmetrically with respect to the borehole, is allowed to take any particular orientation and has a constant opening. The numerical solution for the deformation and strains due to arbitrarily shaped fracture geometry can be obtained by numerically integrating equation (1) over the fracture geometry. However, the analytical expressions for the internal deformation and strains due to a point source in an elastic half-space are already available (Okada, 1992). The Okada solution is chosen as it provides simplified closed-form expressions for any arbitrarily oriented shear or tensile fracture. Given the point source solution, a quadrature rule can be used to numerically integrate equation (1) over the fracture geometry by considering the point sources to be located at these quadrature points. The displacement and tilts at an arbitrary point can be obtained as the weighted sum of these point source solutions. If for example, the fracture is of an elliptical shape, the integration can be performed by a change of coordinates from a Cartesian coordinate system to an elliptical (r & θ) coordinates system using the transformation

$$x/a = r\cos(\theta) \quad y/b = r\sin(\theta) \tag{3}$$

where a and b are the semi-major and semi-minor axis of the ellipse respectively, and r varies from 0 to 1. The Gauss-quadrature method can then be used to integrate along each axis to obtain the solution. In the case of polygon shaped fractures, the quadrature points and weights are computed using the algorithm recently developed by (Mousavi et al., 2010) for arbitrary polygons. The salient feature of this algorithm is that it eliminates the need for partitioning the domain into triangles for numerical integration. Further, it can be used both on concave and convex polygons, as well as polygons having a regular or irregular shape. Figure 2 shows the location of quadrature points in a typical polygon shaped geometry obtained using this algorithm. Once the quadrature points and the weights are known, the numerical solution for the displacements and tilts due to polygon shaped DD singularity can be obtained as a weighted sum of the point source solutions as before. The accuracy of the method was verified for the limiting case in which the polygon is a rectangle, in which case the numerical solution can be compared with the closed-form analytical solution.

2.2 Modified extended Kalman filter

The Kalman filter is a predictor-corrector type algorithm that is used to obtain an optimal state estimate of a physical system based on the input signals and observed outputs (from a measurement device). The extended Kalman filter (EKF) (Gelb, 1974) is the nonlinear version of the Kalman filter that linearizes about the current mean and covariance estimate. Consider the physical process with a state vector $x \in R^n$ and governed by the following equation

$$x_k = f(x_{k-1}, u_{k-1}) + w_{k-1} \tag{4}$$

and a measurement $z \in R^n$ defined as

$$z_k = h(x_k) + v_k \tag{5}$$

In equations (4) and (5) above x_k is the state vector at any discrete time k, u_{k-1} is the known input vector, z_k is the measured output, and w_k and v_k correspond to the process and measurement noise respectively. Both the process and measurement noise are assumed to be independent and normally distributed with zero mean and covariance Q_k and R_k respectively. Finally, $f(.)$ and $h(.)$ are non-linear functions relating the past state at the time $(k-1)$ to the current state at the time k, and the current state x_k to the measurement z_k respectively. Both the process and measurement noise are assumed to be additive.

Given the input signal and the measurement data, the EKF estimates the mean and variance of the state vector in a predictor-corrector sequence. The predictor step or the time update equations project the state and the covariance estimate from the previous step to the current step using equation (4) as

$$\begin{aligned} \hat{x}_{k|k-1} &= f\left(\hat{x}_{k-1|k-1}, u_{k-1}\right) \\ P_{k|k-1} &= F_{k-1} P_{k-1|k-1} F_{k-1}^T + Q_{k-1} \end{aligned} \tag{6}$$

The correction step or the measurement update equation updates the state vector after the measurements are taken. This is done by adding a weighted difference of the residual, which is the difference between the actual measurement and the prediction obtained using equation (5), to the state estimate obtained in the prediction step. The weighting factor is the Kalman gain that minimizes the posteriori error covariance. The correction step or the measurement update equations are given as

$$\begin{aligned} K_k &= P_{k|k-1} H_k^T \left(H_k P_{k|k-1} H_k^T + R_k\right)^{-1} \\ \hat{x}_{k|k} &= \hat{x}_{k|k-1} + K_k \left(z_k - h\left(\hat{x}_{k|k-1}\right)\right) \\ P_{k|k} &= (I - K_k H_k) P_{k|k-1} \end{aligned} \tag{7}$$

where K_k is the Kalman gain that is an $n \times m$ matrix where n and m correspond to the number of state variables and the number of measurements respectively. Due to the non-linear nature of the process and the measurement relationship, the time update and measurement update equations (6) and (7) use the Jacobian of $f(.)$ and $h(.)$ to linearize the estimates about (4) and (5) and are given as

$$F_{k-1} = \frac{df}{dx}\Big|_{\hat{x}_{k-1|k-1}, u_{k-1}} ;\ H_{k-1} = \frac{dh}{dx}\Big|_{\hat{x}_{k-1|k-1}} \tag{8}$$

The EKF algorithm described above is an unconstrained state estimation scheme. Constrained state estimation is often important when simulating engineering systems to get physically meaningful results. The constraints mainly arise due to physical limitations on the possible values the state parameters may take (e.g. the fracture opening has to be positive). In the inverse problem discussed in this paper, we are mainly interested in a box type constraint wherein the state parameters could take any value within a physically permissible range. A number of methods have been proposed to deal with constrained state estimation such as the moving horizon estimation (Rao et al., 2003), recursive non-linear dynamics data reconciliation (Vachhani et al., 2005) and constrained particle filters (Shao et al., 2010). These methods however require an optimization problem to be solved in every step, which requires a higher computational effort. Recently (Prakash et al., 2014) have proposed an optimization free modified extended Kalman filter to handle box type constraints. They have proposed two schemes both of which use a truncated multivariate normal distribution to approximate the prior and posterior distributions. We have used one of those schemes to constrain the state parameters in our model. The basic idea of this method is to first draw a set of random samples from a multivariate Gaussian distribution $N(\mu, \Sigma)$ with an assumed initial mean (μ) and covariance matrix (Σ) for the state variables. The samples that fall outside the permissible range $(x_L \leq x \leq x_U)$, with the subscripts denoting the upper and lower limit respectively, are then ignored. The mean and covariance matrix of the truncated distribution is then computed and used in further computations. If we consider the prediction or process update step (6), the samples are generated from the multivariate Gaussian distribution $N\left(\hat{x}_{k|k-1}, P_{k|k-1}\right)$ as

$$\hat{x}^{(i)}{}_{k|k-1} = \hat{x}_{k|k-1} + \left(P_{k|k-1}\right)^{0.5} \gamma^i, \quad \gamma^i \sim N(0, I) \ \ i = 1,2, \ldots N \tag{9}$$

The constrained samples $\bar{x}_c^{(i)}{}_{k|k-1}$ are then obtained by picking those points which are within the permissible range. The mean and variance of this constrained sample is then computed as

$$\hat{x}_{c_{k|k-1}} = \frac{1}{N} \sum_{i=1}^{N} \bar{x}_c^{(i)}{}_{k|k-1} \tag{10}$$

$$P_{c_{k|k-1}} = \frac{1}{N-1} \sum_{i=1}^{N} \left(\bar{x}_c^{(i)}{}_{k|k-1} - \mathbf{1}\hat{x}_{c_{k|k-1}}\right)^T \left(\bar{x}_c^{(i)}{}_{k|k-1} - \mathbf{1}\left(\hat{x}_{c_{k|k-1}}\right)^{\mathrm{T}}\right) \tag{11}$$

where $\mathbf{1}$ is an $\mathrm{N} \times 1$ vector of 1's. The constrained mean and covariance matrix $\left(\hat{\mathrm{x}}_{\mathrm{c_{k|k-1}}}, \mathrm{P}_{\mathrm{c_{k|k-1}}}\right)$ are now used to update step (7) to obtain the posterior. The above procedure ((9)-(11)) is also repeated after the update step (7), except that the samples points are now drawn from the posterior $N\left(\hat{x}_{k|k}, P_{k|k}\right)$.

3. RESULTS AND DISCUSSIONS

In this section, the results obtained by inverting synthetic and field data sets are presented. In both cases, the displacement discontinuity method discussed in section 2.1 is used as the forward model and the posterior distribution of the fracture parameters, namely the fracture dip, dip orientation opening, and geometric parameters, are obtained using the modified extended Kalman filter. The synthetic data sets were used to validate the model, and the applicability of the model is demonstrated by using it to invert data from preconditioning fracturing trails carried out at the site.

3.1 Synthetic Example

The synthetic data sets were generated for a polygon shaped fracture propagating asymmetrically with respect to the borehole, in an elastic half-space. The fracture is assumed to have a constant opening, dip and dip orientation throughout. An array of twelve tiltmeters is assumed to be located on a plane 1m below the ground surface to record the tilt signals. Twelve tiltmeters were chosen as the actual field trials typically used 10-12 tiltmeter for monitoring the fracturing treatment. The injection point is assumed to be located 50m below the ground surface, and its location is chosen such that measurements satisfy both near-field and far-field conditions, as the fracture propagates. Near and far-field conditions are determined based on the resolution index, defined as the distance d between the tiltmeter and the fracture center, and characteristic half length of the fracture l. If the value of the resolution index is greater than three, the measurements are termed as far-field measurements, as the distance between the fracture center and the measurement location is much larger than the characteristic dimension of the fracture (Lecampion et al., 2005). In the case of fractures with irregular shapes such the polygon model shown in Fig. 1, the characteristic length of the fracture is taken as the average of all fracture dimensions. The fracture dimensions are assumed to increase at some known rate over six discrete time intervals. The growth rate is chosen in such a way that initially the measurements are in the far-field and as the fracture propagates and its characteristic length increases the measurements satisfy near field conditions. Also the fracture is assumed to propagate asymmetrically with respect to the injection point. With the fracture dimensions known at every step, the forward model discussed in section 2 is used to compute the tilt components at the tiltmeter locations, and the data is collected over all the six time instances. A Gaussian noise $N(0, \sigma^2)$ component, with a standard deviation σ that equals 10% of the observed standard deviation of the computed tilt vector, is added to the synthetic data to mimic actual field conditions. The forward model and the modified Kalman filter are then used to determine the fracture parameters from the noisy data. While using the extended Kalman filter, it is assumed that the fracture parameters do not change with time, or in other words there is no change in the state variables from the time $(k-1)$ to k in the prediction step shown in equation (6) except for any contribution from the noise component. The quadrature points within the polygon geometry are generated using the algorithm developed by (Mousavi et al., 2010) as mentioned before. Figure 2 shows the distribution of quadrature points obtained using the algorithm, with a quadrature rule of degree 10.

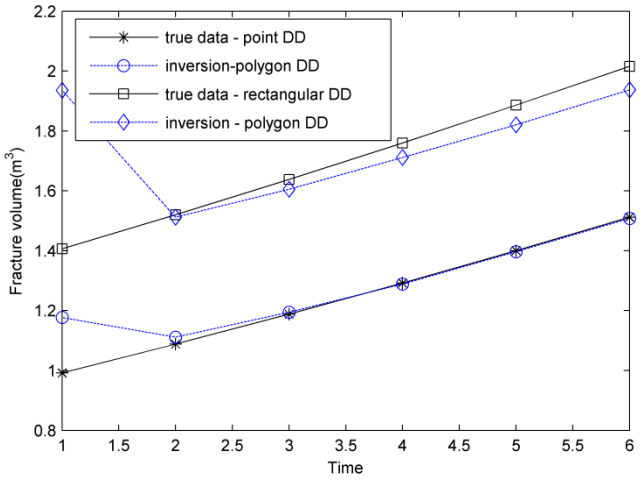

Figure 3 Comparison of true vs. estimated fracture volume when using a point DD and rectangular DD singularity as forward models and an polygon DD model for inversion. In this comparison the injection point is 150m below the ground surface to simulate far field conditions.

To validate our model we first check to see if it can recover the fracture volume when used to invert far field data. DD models of any given geometry would produce similar tilt vectors when the measurements are in the far-field (Lecampion et al., 2005). Hence, under far field conditions any forward model should be able to predict the fracture volume with reasonable accuracy, even thought the geometric parameters obtained by inversion may not be correct. To verify this fact, a point DD and rectangular DD singularity were used as the forward model for generating the tilt signal as described before, and the polygon DD singularity was used as the forward model to invert the data. The closed-form analytical solution for the displacement and strains due to a rectangular DD singularity developed by (Okada, 1992) is used for computing the tilt vector. To avoid near field conditions the injection point is assumed to be located 150m below the ground surface (Figure 1) in this case. The results of the simulation is shown in Figure 3 and it can be observed that there is good agreement between the true volumes generated using the rectangular or point DD forward model and fracture volumes predicted using the polygon DD model, as expected. The generated volumes are different so that the data and the comparison can be more easily displayed in Figure 3.

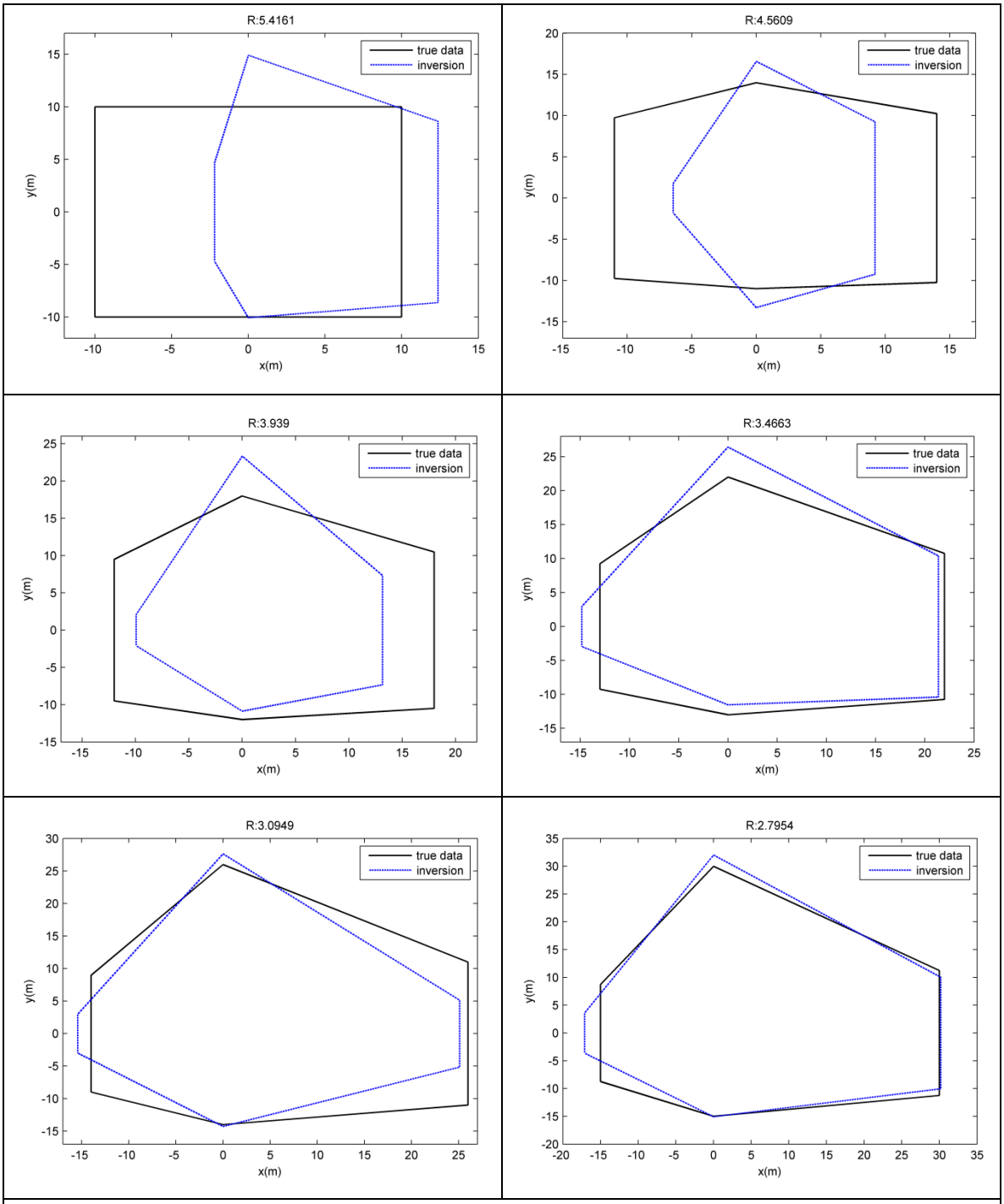

Figure 4 Comparison of true vs. the predicted fracture geometry for the polygon DD model. In this comparison the injection point is 50m below the ground surface and the value of R, the resolution index, that applies to each case are given.

The fracture parameters obtained by the inverting the synthetic data using the polygon DD model is shown in Figure 4. The figure shows the comparison between the actual or true fracture geometry used to generate the tilt vector and the geometry predicted by inversion. To reiterate, the injection point was assumed to be located 50m below the ground surface in the following discussions. The resolution index value that changes as the fracture evolves is also given. It can be observed that the error or the difference between the true and predicted fracture geometries is much higher at the beginning as the resolution index is large. However, the error decreases significantly, as the fracture grows and the resolution index decreases. As mentioned earlier the fracture growth is asymmetric. This asymmetry is characterized using the asymmetric ratio $\mathrm{AR} = \mathrm{L2}/\mathrm{L1}$ or $\mathrm{H2}/\mathrm{H1}$, defined as the ratio of fracture dimensions on either side of the borehole (refer to Fig 1) along the x and y directions. One of the objectives of developing this inversion model was to see how well the fracture asymmetry can be captured from tiltmeter measurements. Figure 5 shows the comparison between the true and predicted values of AR. It can be observed that the predicted AR along the x direction is offset by a large margin in the beginning. However the error significantly drops as the fracture propagates, with errors dropping below 12% as the simulation progresses. At the start of the simulation, the limited prior information and measurements are unable to provide a correct estimate of the fracture parameters. As the fracture propagates, the state estimate gets closer to the actual value and

therefore the predicted AR gets closer to the actual value. The dip angle and dip direction influence the generated tilt vectors both under far field and near field conditions, and therefore these parameters must be recovered accurately under both near and far field conditions. In the current example, a dip angle of 30^0 and a dip orientation 160^0 were used to generate the synthetic data set. These values were successfully recovered from the inversion with a maximum error of less than 10%, further validating the model.

Finally, Figure 6 shows a pictorial representation of the correlation matrix wherein the off diagonal elements show the degree of correlation between the fracture parameters of the polygon model. The values indicate the degree of linear relationship between the variables, and values close to ± 1 show strong correlation between the variables. It can be observed that the geometric parameters L, H, δ show high correlation. As the fracture volume is constant at a given time, a change in one of the geometric parameters is compensated by a corresponding change in the other variable to maintain the volume constant. In comparison the fracture angles (dip and dip orientation) and geometric parameters have lesser correlation.

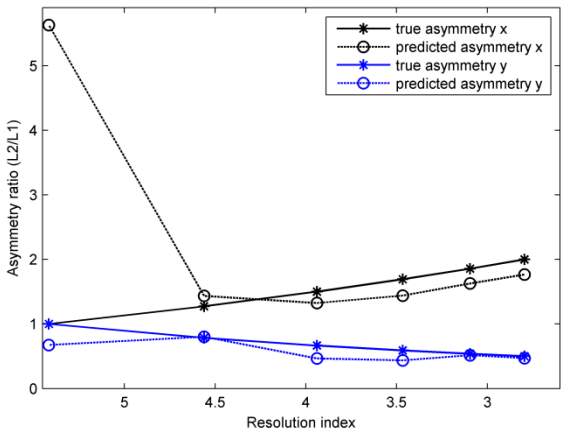

Figure 5 Comparison of true and predicted asymmetry for the polygon model.

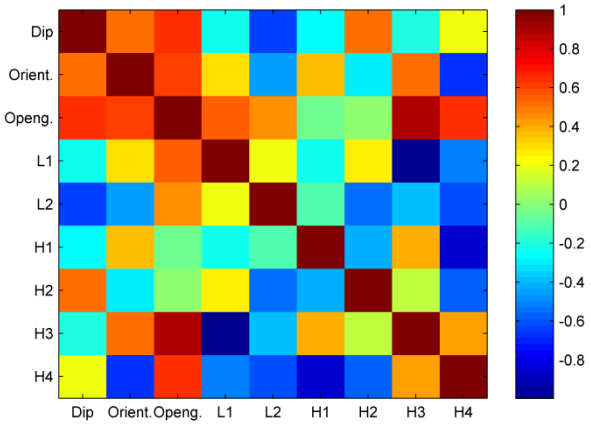

Figure 6 Matrix plot showing the correlation between different fracture parameters for the polygon DD model

3.2 Field Problem

The field data were obtained from preconditioning field trials carried out by CSIRO at the Narrabri coal mine, New South Wales, Australia. In underground coal mining, the region in front of the coalface is supported by a series of hydraulic roof supports that are moved forward along the longwall face and the roof immediately above the seam is allowed to cave into the mined out goaf or void region behind the supports. If the roof is strong, caving might not occur until a large amount of coal has been extracted and a sudden failure can cause the loads on the supports to increase significantly with potential for a wind blast to be generated. Preconditioning using hydraulic fracturing is a rock caving control technique in which hydraulic fractures are propagated in the rock mass to promote earlier caving. The fractures weaken the otherwise massive roof rock so that it will cave sooner and more uniformly, which significantly improves the safety conditions at the site (Jeffrey et al., 2013). The major objective of the preconditioning trials at Narrabri was to ascertain if multiple parallel horizontal fractures with a vertical spacing of 2.5m could be formed and extended to a distance of 30m from the borehole. The treatment consisted of five fractures spaced 2.5m apart, generated using a straddle packer system injecting water at the rate of 100-400 L/min, at a depth of 140-160m. The treatments were monitored using offset boreholes drilled between 10-30m from the injection hole, stress change monitoring instruments, and an array of 10-12 tiltmeters placed 10m below the ground surface in shallow boreholes.

The measurements obtained from offset boreholes confirmed that the fractures were nearly horizontal (Jeffrey et al., 2013). This served as a reference to compare the results from the inverse analysis and study its effectiveness in predicting fracture parameters. The measured tilt signals are obtained in a raw format and contain considerable noise, which are signals that do not correspond to the actual fracturing treatment such as earthquakes, instrument drift or tidal movements. To improve the signal to noise ratio, the data is first filtered using a Savitzky-Golay filter (Press, 2007). Random spikes are then manually removed and substituted with an approximate local signal, and finally low-frequency noise is removed by a detrending process, wherein the trend obtained by fitting a low frequency function to the signal is subtracted from the denoised signal. The extracted signal is then used for inversion. As the fractures were expected to grow asymmetrically in a radial direction, an elliptical DD forward model was chosen and the inversion was carried out using the modified extended Kalman filter discussed in the previous section. As the pressurized fluid creates opening mode fractures in the rock mass, only the normal component of the displacement jump in Eq. 1 is considered for computing the displacement and tilt, and the fracture opening (δ) is assumed to be constant. As mentioned in Section 3.2, the modified extended Kalman filter used in this work uses a box type constraint to obtain physically meaningful results. In this case the dip, dip orientation and fracture opening were constrained within a range of 0-60^0, 0-180^0, and 0-3mm respectively. Given the knowledge of the injected fluid volume, approximate upper bounds on the fracture geometries $(R1, R2, R3)$ were obtained by assuming some reasonable treatment efficiency. In hydraulic fracturing, the treatment efficiency is defined as the ratio of the actual fracture volume to the actual volume of injected fluid. The treatment efficiency accounts for all fluid losses during the fracturing treatment and is typically between 50-70% (Chen and Jeffrey, 2009). As the amount of fluid injected into the well is known, a rough estimate of the fracture volume can be obtained by assuming some prior treatment efficiency. Again this assumes that fractures are perfectly radial. To account for the fractures developing asymmetrically, the estimates can be appropriately scaled. As before, it is assumed that the fracture parameters do not change with time during the fracturing treatment, or in other words there is no change in the state variables from the time $(k-1)$ to k in the prediction step shown in equation (6) except for any contribution

from the noise component. The process noise covariance matrices Q and the measurement noise covariance R were assumed to be constant diagonal matrices with a variance of 0.6 and 0.05 respectively. The justification for using a higher variance for matrix Q is that we have limited knowledge about how the fracture parameters evolve with time and the higher value quantifies this uncertainty, while it is assumed that the measurements are reliable and therefore R is assigned a smaller value.

Table 1 Fracture parameters estimated by the elliptical DD model

Frac. No.	Estimated fracture parameters						Estimated variance					
	φ	θ	δ (mm)	R1 (m)	R2 (m)	R3 (m)	φ	θ	δ (mm)	R1 (m)	R2 (m)	R3 (m)
1J	3.15	26.8	2.89	27.8	17.3	21.1	1.9	0.09	0.21	7.2	5.9	6.9
2J	2.31	29.3	2.88	29.1	9.8	23.6	1.8	0.11	0.23	8.68	7.1	7.3
4J	2.36	21.9	2.84	24.4	17.6	19.1	4.3	0.12	0.32	9.4	8.4	9.8

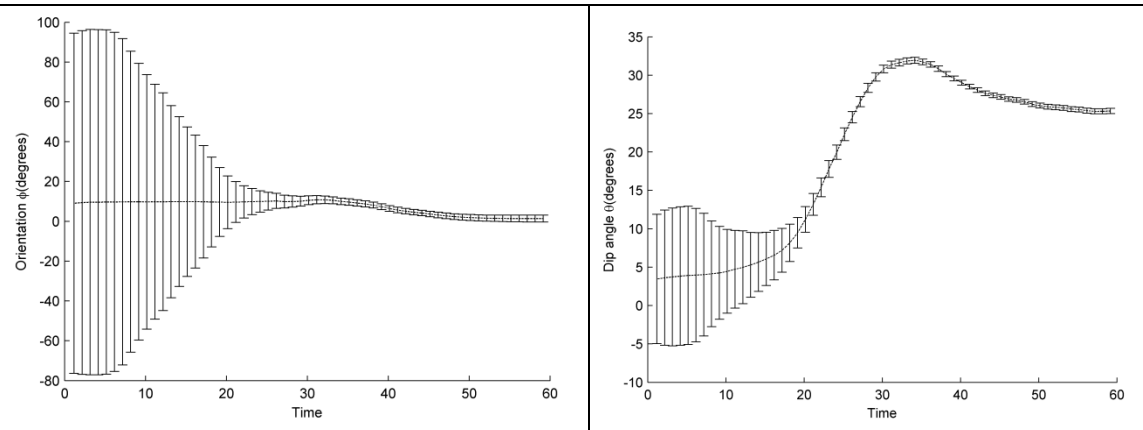

Figure 7 Evolution of the predicted fracture strike and dip angles during the fracturing treatment for fracture F01 at borehole J. The injection point is at (0, 0,-146.8m).

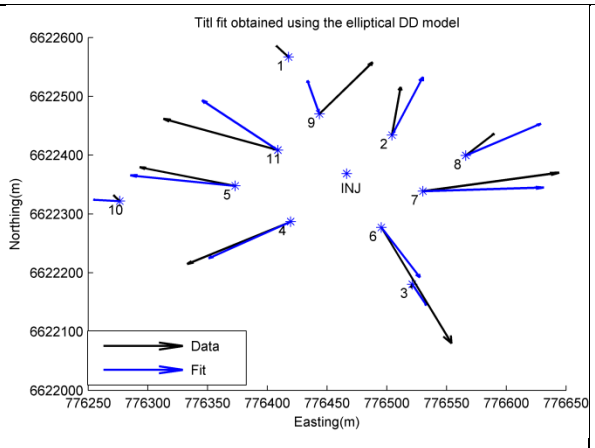

Figure 8 Comparison of the measured tilt signal vs. the tilt fit obtained by inversion for Fracture 01 at borehole J. The injection point is at (0,0,-146.8m)

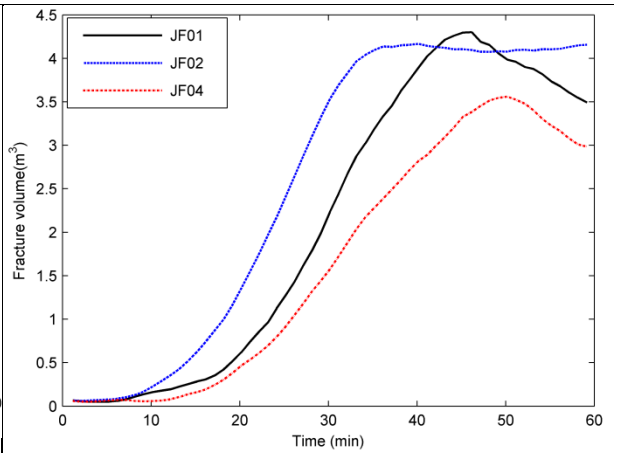

Figure 9 Estimated fracture volume for different fractures (J refers to the borehole and F01 is the fracture number).

Data collected from fracturing treatment carried out at a depth of 146.8, 149.3 and 151.8m in borehole J were analyzed. Inversions were carried out using the extracted tilt signals over the entire injection phase of about 60min and the fracture parameters obtained by inversion are summarized in Table 1. The measurements were all in the far field with resolution index exceeding 9. As a result the geometric parameters estimated by inversion showed large variance and the results were not very reliable. In the synthetic example presented before it was shown that the inversion provides better estimates for the fracture dip and dip orientation irrespective of whether the measurement satisfy near field or far field conditions. The evolution of dip and dip orientation of

fracture 1J during the fracturing treatment is shown in Figure 7, together with the observed variance. It can be observed that the variance drops significantly with time from the initially assumed values, indicating that the Kalman filter has converged. In the present case the fractures were expected to be nearly horizontal, which was confirmed from the intersection data from offset bore holes and by temperature logging (Jeffrey et al., 2013). In the case of horizontal fractures, dip orientation does not have any meaning as fractures with different dip orientations will be indistinguishable and therefore produce identical tilt vectors. The dip estimates are therefore of greater interest.

As seen in Table 1, the fracture dip values have smaller variance and show that the fractures were all sub-horizontal with an average fracture dip of around 26^0. Analysis of tiltmeter data measured from other boreholes in the area predicted an average fracture dip of 16^0 (Jeffrey et al., 2013). Though the dip angles predicted by the model are higher, they are still better than the earlier dip estimates of 38^0 obtained (Jeffrey et al., 2013) using a point DD singularity with fracture center offset as the forward model and a Bayesian inversion procedure. In this case the fracture centre offset is not required and therefore any error introduced in the dip estimate due to incorrect offset estimation is avoided. Computationally, the inversion carried out using the extended Kalman filter is much faster than the Bayesian inversion procedure used in the earlier work (Jeffrey et al., 2013). To invert the measurements taken over a 60min interval, the Bayesian method requires about $575s$ on a standard desktop machine (Intel i5 processor, 2.8GHz and 4GB RAM) while the same procedure takes less than $30s$ when using the extended Kalman filter approach. This can be significant when using the polygon DD forward model as it has more geometric features than the elliptical model. Figure 8 shows the measured tilt vectors vs. the estimated tilt vectors for one of the fractures and it can be seen that the elliptical DD model is able to reasonably fit the observed tilt data, given that the measurements are mainly in the far field regime. Finally, Figure 9 shows the fracture volume estimated by the model for the three different fractures. The volume increases from the start of fracture initiation and reaches it maximum toward the end of the injection phase and drops down during the shut-in period. In the case of fracture 1J, it can be seen that volume reaches its peak at 46min, which agrees well with the actual site information where the fluid injection was carried out for 45min and then shut off. The estimated treatment efficiency was between 30-70%, which is within the range observed for similar preconditioning treatments (Chen and Jeffrey, 2009).

4. CONCLUSION

In this work, we proposed a procedure for inverting tiltmeter measurements using a forward model based on the displacement discontinuity method and modified extended Kalman filter. In comparison to methods that use forward models based on symmetric DD models, the current method is able to model asymmetric fracture of any general shape, and also eliminates the need for estimating center offset. The results obtained by inverting synthetic data showed that the model is able to successfully recover the fracture dip and dip orientation under all conditions with reasonable accuracy, and the geometric parameters when the measurements are in the near field. The applicability of the method was finally demonstrated by using it to invert data from preconditioning fracturing trails carried out at a mining site. As the measurements were in the far field and the fractures were expected to be nearly horizontal, only the dip estimates from the inversion were useful. It was observed that the dip estimates were greater than close to zero dip angles observed from offset borehole measurements and stress change monitoring. However, they were much better than the earlier estimates obtained using symmetric DD models with center offsets. In conclusion, the proposed model provides improved estimates for fracture dip and orientation under far field conditions, and can provide useful information on the development of asymmetric fractures when measurements satisfy the near field conditions.

REFERENCES

Bennett, C.O., Rosato, N.D., Reynolds, A.C., and Raghavan, R. Influence of Fracture Heterogeneity and Wing Length on the Response of Vertically Fractured Wells. SPE-9886-PA, (1983).

Chen, Z.R., and Jeffrey, R.G. Tilt Monitoring of Hydraulic Fracture Preconditioning Treatments. 43rd U.S. Rock Mechanics Symposium & 4th U.S. - Canada Rock Mechanics Symposium, (2009).

Converse, G., and Comninou, M. Dependence on the elastic constants of surface deformation due to faulting. Bulletin of the Seismological Society of America, 65, (1975), 1173–1176.

Crouch, S.L., and Starfield, A.M. Boundary element methods in solid mechanics: with applications in rock mechanics and geological engineering (London; Boston: Allen & Unwin).

Davis, P.M. Surface deformation associated with a dipping hydrofracture. Journal of Geophysical Research: Solid Earth, 88, (1983), 5826–5834.

Economides, M.J., and Nolte, K.G. Reservoir stimulation (Chichester, England; New York: Wiley).

Gelb, A. Applied Optimal Estimation (MIT Press).

Jeffrey, R.G. Asymmetrically propped hydraulic fractures. Old Production & Facilities, (1996).

Jeffrey, R.G., Chen, Z.R., Mills, K.W., and Pegg, S. Monitoring and Measuring Hydraulic Fracturing Growth During Preconditioning of a Roof Rock over a Coal Longwall Panel. In Effective and Sustainable Hydraulic Fracturing, R. Jeffrey, ed. (InTech), (2013).

Kear, J., White, J., Bunger, A.P., Jeffrey, R., and Hessami, M.-A. Three dimensional forms of closely-spaced hydraulic fractures. In Effective and Sustainable Hydraulic Fracturing, R. Jeffrey, ed. (InTech), (2013).

Lecampion, B., and Gunning, J. Model selection in fracture mapping from elastostatic data. International Journal of Solids and Structures, 44, (2007), 1391–1408.

Lecampion, B., Jeffrey, R.G., and Detournay, E. Resolving the Geometry of Hydraulic Fractures from Tilt Measurements. Pure and Applied Geophysics, 162, (2005), 2433–2452.

Love, A.E.H. A Treatise on the Mathematical Theory of Elasticity (Cambridge University Press).

Mousavi, S.E., Xiao, H., and Sukumar, N. Generalized Gaussian quadrature rules on arbitrary polygons. International Journal for Numerical Methods in Engineering, 82, (2010), 99–113.

Okada, Y. Surface deformation due to shear and tensile faults in a half-space. Bulletin of the Seismological Society of America, 75, (1985), 1135–1154.

Okada, Y. Internal deformation due to shear and tensile faults in a half-space. Bulletin of the Seismological Society of America, 82, (1992), 1018–1040.

Olson, J.. E., Du, Y., and Du, J. Tiltmeter data inversion with continuous, non-uniform opening distributions: A new method for detecting hydraulic fracture geometry. International Journal of Rock Mechanics and Mining Sciences, 34, (1997), 236.e1–236.e10.

Portier, S., Vuataz, F.-D., Nami, P., Sanjuan, B., and Gérard, A. Chemical stimulation techniques for geothermal wells: experiments on the three-well EGS system at Soultz-sous-Forêts, France. Geothermics, 38, (2009), 349–359.

Prakash, J., Huang, B., and Shah, S.L. Recursive constrained state estimation using modified extended Kalman filter. Computers & Chemical Engineering, 65, (2014), 9–17.

Press, W.H. Numerical recipes: the art of scientific computing (Cambridge [u.a.: Cambridge Univ. Press).

Rao, C.V., Rawlings, J.B., and Mayne, D.Q. Constrained state estimation for nonlinear discrete-time systems: stability and moving horizon approximations. IEEE Transactions on Automatic Control, 48, (2003), 246–258.

Riahi, A., and Damjanac, B. Numerical study of hydro-shearing in geothermal reservoirs with a pre-existing discrete fracture network. In Thirty-Eighth Workshop on Geothermal Reservoir Engineering, Stanford, CA, (2013).

Rodriguez, F., Cinco-Ley, H., and Samaniego-V., F. Evaluation of Fracture Asymmetry of Finite-Conductivity Fractured Wells. SPE-20583-PA, (1992).

Shao, X., Huang, B., and Lee, J.M. Constrained Bayesian state estimation – A comparative study and a new particle filter based approach. Journal of Process Control, 20, (2010), 143–157.

Tester, J.W., Anderson, B., Batchelor, A., Blackwell, D., DiPippo, R., Drake, E., Garnish, J., Livesay, B., Moore, M.C., and Nichols, K. The future of geothermal energy: Impact of enhanced geothermal systems (EGS) on the United States in the 21st century. Massachusetts Institute of Technology, (2006), 209.

Vachhani, P., Rengaswamy, R., Gangwal, V., and Narasimhan, S. Recursive estimation in constrained nonlinear dynamical systems. AIChE Journal, 51, (2005), 946–959.

Yang, X., and Davis, P.M. Deformation due to a rectangular tension crack in an elastic half-space. Bulletin of the Seismological Society of America, 76, (1986), 865–881.